Molecular Genetics and Metabolism Reports 1 (2014) 378–390

Contents lists available at ScienceDirect

Molecular Genetics and Metabolism Reports

journal homepage: http://www.journals.elsevier.com/molecular-genetics-and-metabolism-reports/

The retarded hair growth (*rhg*) mutation in mice is an allele of ornithine aminotransferase (*Oat*)

Jason J. Bisaillon, Legairre A. Radden II, Eric T. Szabo, Samantha R. Hughes, Aaron M. Feliciano, Alex V. Nesta, Belinda Petrovic, Kenneth M. Palanza, Dainius Lancinskas, Theodore A. Szmurlo, David C. Artus, Martin A. Kapper, James P. Mulrooney, Thomas R. King *

Biomolecular Sciences, Central Connecticut State University, 1615 Stanley Street, New Britain, CT 06053, USA

ARTICLE INFO

Article history:
Received 7 July 2014
Received in revised form 14 August 2014
Accepted 15 August 2014
Available online 16 September 2014

Keywords:
Alopecia
Positional candidate approach
Gyrate atrophy of the choroid and retina
Complementation testing
Intraspecific backcross mapping

ABSTRACT

Because of the similar phenotypes they generate and their proximate reported locations on Chromosome 7, we tested the recessive retarded hair growth (*rhg*) and frizzy (*fr*) mouse mutations for allelism, but found instead that these defects complement. To discover the molecular basis of *rhg*, we analyzed a large intraspecific backcross panel that segregated for *rhg* and restricted this locus to a 0.9 Mb region that includes fewer than ten genes, only five of which have been reported to be expressed in skin. Complementation testing between *rhg* and a recessive null allele of fibroblast growth factor receptor 2 eliminated *Fgfr2* as the possible basis of the retarded hair growth phenotype, but DNA sequencing of another of these candidates, ornithine aminotransferase (*Oat*), revealed a G to C transversion specifically associated with the *rhg* allele that would result in a glycine to alanine substitution at residue 353 of the gene product. To test whether this missense mutation might cause the mutant phenotype, we crossed *rhg*/*rhg* mice with mice that carried a recessive, perinatal-lethal, null mutation in *Oat* (designated Oat^{Δ} herein). Hybrid offspring that inherited both *rhg* and Oat^{Δ} displayed markedly delayed postnatal growth and hair development, indicating that these two mutations are allelic, and suggesting strongly that the G to C mutation in *Oat* is responsible for the retarded hair growth phenotype. Comparisons among +/+, +/*rhg*, *rhg*/*rhg* and *rhg*/Oat^{Δ}

* Corresponding author. Fax: +1 860 832 3562.
E-mail address: kingt@ccsu.edu (T.R. King).

http://dx.doi.org/10.1016/j.ymgmr.2014.08.002

mice showed plasma ornithine levels and ornithine aminotransferase activities (in liver lysates) consistent with this assignment. Because histology of 7- and 12-month-old *rhg*/*rhg* and *rhg*/*Oat*$^{\Delta}$ retinas revealed chorioretinal degeneration similar to that described previously for *Oat*$^{\Delta}$/*Oat*$^{\Delta}$ mice, we suggest that the *rhg* mutant may offer an ideal model for gyrate atrophy of the choroid and retina (GACR) in humans, which is also caused by the substitution of glycine 353 in some families.

1. Introduction

Spontaneous mutations often provide phenotypes that are distinct from and therefore uniquely informative compared to engineered null alleles of the same genes. For example, our laboratory has recently used a positional-cloning approach to identify a defect in the *Prss8* gene (protease serine S1 family member 8, or prostasin) as the molecular basis of the spontaneous mouse frizzy mutation (formerly *fr*, now designated *Prss8*^{fr}), which generates curly whiskers in homozygotes [1]. These mutants are more mildly affected than *Prss8* knock-outs, which die by 24 h of age (before much hair or skin development can be observed) [2]. Use of *fr* alone or in combination with null alleles of *Prss8* has produced viable mutants that have facilitated, for example, the discovery of new components of the prostasin-matriptase proteolytic signaling cascade, whose normal regulation is necessary at multiple stages in development [3–5]. Similarly, mice homozygous for the spontaneous juvenile alopecia mutation (*jal*) show patchy hair loss [6,7] quite distinct from the complete absence of hair development displayed by the allelic *Gata3* knock-outs [8–12], and will likely provide a unique model for particular non-inflammatory focal alopecias that result from stem-cell loss, rather than a failure of hair-follicle differentiation.

Here we focus on another spontaneous recessive mutation, called retarded hair growth (abbreviated *rhg*) [13], that has been genetically mapped by another group between microsatellite markers *D7Mit206* and *D7Mit105* [14], a span that includes *Prss8*. While *rhg*/*rhg* homozygotes appear normal at birth, by 10 days of age they are smaller than their heterozygous littermates, and display a marked delay in hair development (see Fig. 1). In spite of the similar phenotypes they generate and their similar map positions, *fr* and *rhg* have never been tested for allelism.

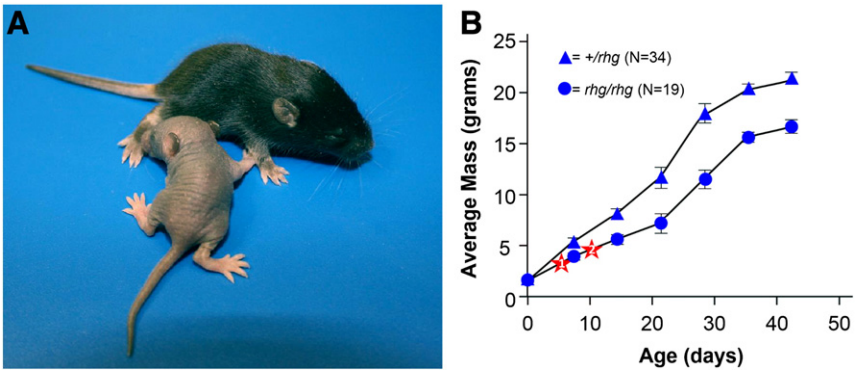

Fig. 1. The phenotype of mutant (homozygous *rhg*/*rhg*) and wild type (heterozygous +/*rhg*) testcross progeny. (A) Mice shown are littermates at 10 days of age. (B) Five testcross litters were weighed together on their day of birth since mutant and wild type pups were indistinguishable at that time. By day 7, progeny could easily be divided into mutant and wild type categories and individual mice were weighed separately and at weekly intervals for 42 days. The average mass (in grams) for as many as 19 mutants and 34 wild type heterozygotes are shown, ± 1 standard deviation. One mutant mouse had died by day six, and two more died by day ten (shown by red stars).

Here we used complementation testing to resolve the genetic relationship between *rhg* and *fr*, and we characterized a large backcross panel of mice to map *rhg* into a different interval on Chromosome (Chr) 7 than has been previously reported. One skin-expressed gene candidate in this corrected interval, *Oat* (for ornithine aminotransferase), was found by DNA sequencing analysis to harbor a transversion mutation that is specific to *rhg*, and is predicted to cause the substitution of an alanine for a highly-conserved glycine. Furthermore, a recessive, engineered null allele (designated Oat^{Δ} herein) failed to complement *rhg*, suggesting that *rhg* is an allele of *Oat* and that the missense mutation we describe is the likely cause of the retarded hair growth phenotype. Finally, physiological evaluation of mice with various *rhg*, Oat^{Δ}, and + genotypes demonstrates, again, that the spontaneous variant may provide a superior model for some forms of ornithine aminotransferase (OAT) deficiency than the engineered null allele.

2. Materials and methods

2.1. Mice

All animals were housed and fed according to Federal guidelines, and the Institutional Animal Care and Use Committee at CCSU approved of all procedures involving mice. Mice from the standard inbred strains A/J and C57BL/6J, inbred FS/EiJ mice (homozygous for the recessive frizzy mutation, *fr*) and segregating inbred B6Ei;AKR-*rhg* mice were obtained from The Jackson Laboratory (Bar Harbor, ME, USA). DNA samples from mouse strains that we do not maintain in our colony were obtained from The Jackson Laboratory's Mouse DNA Resource. Mice homozygous for mutant *fr* alleles were identified by the curly appearance of their vibrissae, which is apparent one to two days after birth and persists throughout life. Mice homozygous for mutant *rhg* alleles were produced in test crosses, and were most reliably identified at 7 to 10 days of age by their smaller body size, disorganized vibrissae and delayed hair development, compared to wild type littermates (see Fig. 1A). Although some *rhg*/*rhg* mutants die by weaning age, survivors become increasingly harder to distinguish from wild type littermates and by 10 weeks of age wild and mutant mice can be quite similar in appearance. Among pigmented mice, *rhg* homozygotes can sometimes be distinguished from age-matched heterozygotes because the tips of some guard hairs are white, giving their coats a “dusty” appearance.

Mice carrying a targeted null mutation in the fibroblast growth factor receptor 2 gene (herein designated $Fgfr2^{\Delta}$) were produced by crossing males homozygous for the “floxed” $Fgfr2^{tm1Dor}$ allele (The Jackson Laboratory, stock #007579)[15] to females homozygous for a cre recombinase (*cre*) transgene under the control of the adenovirus *EIIa* promoter (The Jackson Laboratory, stock #003724) [16]. Widespread (including germ-line) expression of cre recombinase in the resulting early F_1 embryos caused excision of the *loxP*-flanked exons 8–10 of the $Fgfr2^{tm1Dor}$ allele, deleting sequences that encode the alternatively-spliced, immunoglobulin-like (Ig) domains IIIb and IIIc, as well as the transmembrane (TM) domain of Fgfr2 protein. Fully viable and fertile heterozygous ($Fgfr2^{+}/Fgfr2^{\Delta}$) mice were maintained by crossing $Fgfr2^{\Delta}$ carriers to C57BL/6J. To identify the various *Fgfr2* alleles, we used the three-primer PCR assay described by Yu et al. [15]. For this test, primer pair F1 (5′ ATAGGAGCAACAGGCGG 3′) and R1 (5′ TGCAAGAGGCGACCAGTCAG 3′) produced a 142 bp amplimer from wild-type, and a 207 bp amplimer from $Fgfr2^{tm1Dor}$ templates. Primer pair F1 and R2 (5′ CATAGCACAGGCCAGGTTG 3′) yielded a 471 bp amplimer from $Fgfr2^{\Delta}$ templates.

Mice carrying the Oat^{tm1Dva} targeted mutation (designated herein as Oat^{Δ}) were kindly provided by Dr. David Valle (Institute of Genetic Medicine and Departments of Pediatrics, Ophthalmology and Molecular Biology & Genetics; The Johns Hopkins University School of Medicine, Baltimore, MD, USA). The creation of the Oat^{Δ} mutation is described by Wang et al. [17]. In brief, Valle *et al.* used homologous recombination to introduce a neomycin-resistance cassette into Exon 3 at Codon 40, which truncates the OAT peptide 13 amino acids downstream of the cleavage site for the N-terminal mitochondrial targeting sequence, resulting in a null allele at the level of enzyme function. Heterozygous (Oat^{+}/Oat^{Δ}) mice are fully viable and fertile, and were maintained by crossing Oat^{Δ} carriers to C57BL/6J. To identify Oat^{+} and Oat^{Δ} alleles, we used the three-primer PCR assay described by Wang et al. [17]. For this test, primer pair F2 (5′ AACTAGCAAGTCTGCAGACC 3′) and R3 (5′ TCCACAAGGCATTCAGTGCG 3′) produced a 280 bp amplimer from wild-type templates. Primer pair F3 (5′ CTGAGGCGGAAAGAACCAG 3′) and R3 yielded a 220 bp amplimer from Oat^{Δ} templates.

2.2. DNA isolation and analysis

Genomic DNA was isolated from tail-tip biopsies taken from two-to-three week old mice using the NucleoSpin® Tissue kit distributed by Clontech Laboratories (Mountain View, CA, USA). DNAs were analyzed by the polymerase chain reaction (PCR) performed in 13 μl reactions using the Titanium® Taq PCR kit, also from Clontech Laboratories, as directed. Single-stranded DNA primers for PCR were synthesized by Integrated DNA Technologies (Coralville, Iowa, USA), based on sequence data from online sources [18,19]. PCR products were visualized by electrophoresis through 3.5% NuSeive® 3:1 Agarose (Lonza, Rockland, ME, USA) gels, stained with 0.5 μg/ml ethidium bromide and photographed under UV light. In addition to standard microsatellite markers [20] on Chr 7, we used 6 DNA markers based on single-nucleotide polymorphisms (SNPs) known to differ between the inbred strains used here [18,19]. These markers (herein designated *SNP1–6*) are described in detail in Supplementary Tables S1 and S2. For DNA sequencing, PCR amplimers were purified and concentrated to about 1.5 μg per 30 μl using the QIAquick® PCR Purification Kit (Qiagen Sciences, Germantown, MD, USA), and shipped to SeqWright Genomic Services (Houston, TX, USA) for primer-extension analysis.

2.3. Plasma amino acid analysis

Blood samples were collected from the retro-orbital plexus of ether-anesthetized mice, and plasma was prepared in the presence of sodium heparin. Plasma was shipped on dry ice to BioSynthesis, Inc. (Lewisville, TX, USA) where samples were analyzed on a Hitachi L-8800 amino acid analyzer after removing proteins by treatment with 40 g/l sulfosalicylic acid/internal standard solution, centrifugation, and filtration. The amino acids were separated by high-resolution ion-exchange chromatography and then subjected to postcolumn ninhydrin derivatization. Detection was by spectrophotometry at 570 nm and 440 nm.

2.4. Arginine supplementation

Arginine supplementation (modified from the protocol previously described by Wang et al. [17,21,22]) was administered to 3–21 day old mice by i.p. injection at 12 hour intervals. The solution injected was 0.33 M arginine hydrochloride and 0.17 M arginine-free base (pH 9) (Sigma-Aldrich, St. Louis MO, USA). The initial dose was 5 mM/kg body weight/injection or about 25 μl per dose for a mouse weighing 2.5 g at 7 days of age. The volume of 0.5 M arginine administered remained constant so that as the animals grew, the dose tapered to approximately 1 mM/kg body weight/injection by 20 days.

2.5. Monitoring the catalytic activity of OAT

Liver tissue (0.45 g) was homogenized (1:10, *w*/*v*) in fractionation buffer consisting of 300 mM sucrose, 5 mM HEPES (pH 7.0), 3 mM dithiothreitol and 0.2 mM EDTA. Homogenates were centrifuged at 600 ×*g* at 4 °C for 10 min. Supernatants were centrifuged at 12,000 ×*g* at 4 °C for 15 min. Pellets were resuspended in 0.5 ml fractionation buffer that contained 5 mM EDTA and were centrifuged again at 600 ×*g* at 4 °C for 10 min, and these supernatants were centrifuged at 4500 ×*g* at 4 °C for 10 min. The mitochondrial pellets were resuspended in 150 μl potassium pyrophosphate (100 mM, pH 8.0) containing NP-40 (2% *v*/*v*), and centrifuged at 5000 ×*g* at 4 °C for 15 min. The resulting supernatants (mitochondrial extracts) were stored at −80 °C until assayed.

OAT activity was assayed by a modification of the method developed by Juncosa, Lee and Silverman [23]. Wells in a 96-well microtiter plate were loaded with 160 μl of a mixture containing 100 mM potassium pyrophosphate (pH 8.0), 10 mM α-ketoglutarate, 0.4 mM NADH, 0.025 mM pyridoxal 5′-phosphate, and 80 mM L-ornithine (all from Sigma-Aldrich, St. Louis, MO, USA). After pre-incubating plates at 37 °C for 10 min, 2 μl recombinant human pyrroline-5-carboxylate reductase 1 (0.5 mg/ml; U.S. Biological, Salem, MA, USA) and 40 μl of mitochondrial extract (as a source of OAT) were added to each well. Absorbance was measured at 340 nm every 10 s for 45 min in a Spectromax 250 late reader running SoftMax Pro software. All assays were performed in triplicate, and at least three mice of each genotype were tested independently. Activities for each sample, in terms of ΔA_{340}/min/mg protein, were

determined by measuring the slope of the linear portion of each dataset (generally between 2–10 min after adding mitochondrial extract). Protein concentrations were quantified by the Bradford method. Average OAT activity for each genotype is shown, ± 1 standard error.

2.6. Histology of retinas

Eyes from 7- or 12-month-old mice were removed after euthanasia, and were fixed by immersion in Davidson's Fixative (Rowley Biochemical Inc., Danvers MA, USA). After 24 h, samples were dehydrated and embedded in paraffin. Seven-μm-thick sections were stained with Lee's Stain (methylene blue and basic fuchsin) and were examined by light microscopy. Images were captured using a SPOT camera (Diagnostic Instruments, Sterling Heights, MI, USA) attached to an inverted Nikon (Melville, NY, USA) microscope.

3. Results

3.1. Complementation testing with *Prss8*^{fr}

To determine if *Prss8*^{fr} and *rhg* might be alleles of the same gene, crosses were conducted to produce mice that carried single copies of both recessive mutations. Typically, when such "doubly-heterozygous" subjects are phenotypically wild type, the two recessive mutations are said to complement and are assumed to be defects in distinct genes. By contrast, if mice inheriting two recessive defects are phenotypically mutant, then the mutations "fail to complement", indicating that they are variant alleles of the same gene. All of the progeny from each of the complementation crosses performed were phenotypically wild type (with normal vibrissae and furry coats, and normal body size at 10 days of age, see Supplementary Table S3), so we conclude that—in spite of the similar phenotypes they control and their similar locations on Chr 7—the recessive *fr* and *rhg* mutations identify distinct genes.

3.2. Low-resolution genetic mapping

The *D7Mit206* to *D7Mit105* interval into which *rhg* has been previously mapped by Curtain et al. [14] includes more than 125 genes [19]. To reduce this number of candidates, we produced a 1462-member

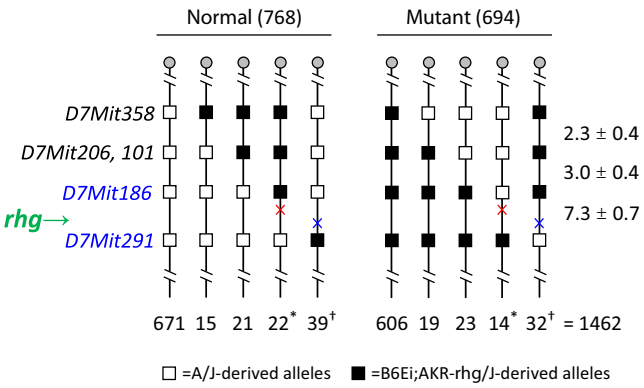

Fig. 2. Segregation of *rhg* and five microsatellite markers on mouse Chr 7 among a large backcross family of mice. To produce these 1462 N_2 generation mice, (A/J X B6;AKR-*rhg*/J)F_1 females were backcrossed to B6;AKR-*rhg*/J homozygous mutant males. The Chr 7 haplotype depicted by the vertical line (the knob at the top of which represents the centromere) was that transmitted by the F_1 dam. The number of backcross mice that inherited each haplotype is shown beneath it. The microsatellite markers typed are shown to the left, and genetic distances (in percent recombination ± 1 standard error) are shown to the right. Open boxes indicate A/J derived alleles; filled boxes represent AKR-derived alleles. The *rhg* mutation is located between *D7Mit186* and *D7Mit291*, since it must lie below the crossovers (depicted in red) carried by the 36 recombinants marked with an asterisk, and above the crossovers (shown in blue) carried by the 71 recombinants marked with a dagger. The deficit of mutants, although not statistically significant ($\chi^2 = 3.746$; $P \approx 0.053$), suggests that *rhg*/*rhg* mice are only partially viable, and survived to phenotyping and DNA sampling (day 10 to 20) only about 90% of the time.

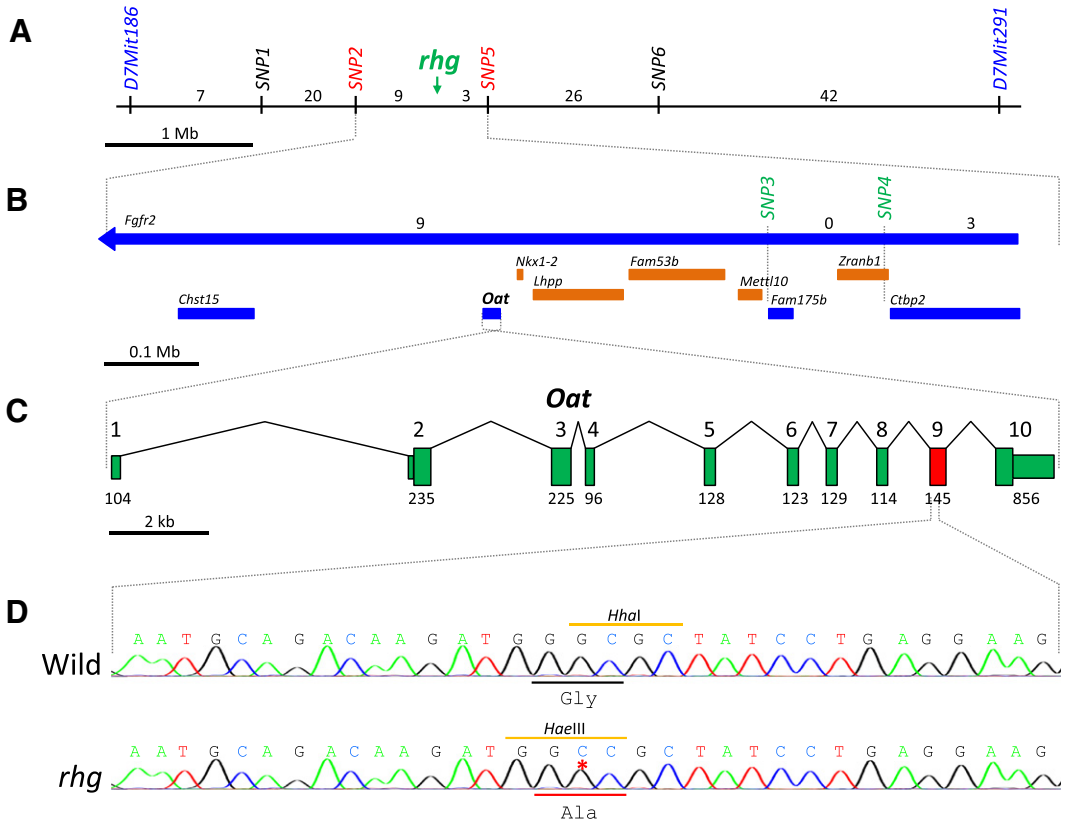

Fig. 3. Physical maps of the "*rhg*-critical" region on mouse Chr 7. (A) The relative positions of four SNP markers are shown for the 5.9 Mb region that is flanked by *D7Mit186* and *D7Mit291* (a 1 Mb scale bar is shown). The number of crossovers identified in each marker interval is shown in red. (B) The interval between *SNP2* and *SNP5* is expanded (a 0.1 Mb scale bar is shown), and the extent of known genes in that region are depicted by rectangles. Those in blue are candidates reported to be expressed in skin. *Fgfr2* extends beyond this region, centromeric to *SNP2*. The relative positions of two SNP markers located inside of this interval are shown, and the number of crossovers identified in each marker-defined sub-interval is indicated in red. (C) The *Oat* gene is expanded (with a 2 kb scale bar) to show its genomic structure. Boxes indicate the 10 exons that comprise *Oat*; shorter boxes represent the 5′ and 3′ untranslated regions. The number below each exon is the number of base pairs each contains. (D) Exon 9 is expanded to show the G to C transversion mutation associated with *rhg* (indicated by the red asterisk). This mutation creates a *Hae*III target site in the mutant and destroys a *Hha*I target site in the wild type allele, and is predicted to change a glycine residue at position 353 of the gene product to alanine.

backcross (N_2) family by crossing (A/J x B6;AKR-*rhg*/J)F_1 females with B6;AKR-*rhg*/J mutant males. These N_2 mice were typed for *rhg* at 10 days and DNA isolated from each mouse at weaning was characterized for five PCR-scorable microsatellite markers that extend beyond, on both flanks, the "*rhg*-critical" interval identified by Curtain et al. [14]. Surprisingly, our analysis indicated that *rhg* actually maps between *D7Mit186* and *D7Mit291* (see Fig. 2), an interval that is nearly 2.1 Mb centromere-distal to that where Curtain et al. had suggested that *rhg* is located.

3.3. Complementation testing with $Fgfr2^{\Delta}$

The *D7Mit186* to *D7Mit291* interval where *rhg* maps overlaps the coordinates of the fibroblast growth factor receptor 2 (*Fgfr2*) gene [19]. *Fgfr2* is known to be expressed in embryonic vibrissae and in the outer root sheath of perinatal hair follicles [24–27]. Furthermore, mutation of *Fgfr2* is known to alter hair morphology, at least when null-allele homozygotes (which die at Theiler Stage 16–19) are rescued to birth by the formation of chimeras with tetraploid embryos, and their skin is transplanted onto nude hosts [28]. To determine if a defect in *Fgfr2* might be the basis of *rhg*, we produced mice that carry a null allele of *Fgfr2* (herein designated $Fgfr2^{\Delta}$, see Materials and methods), and crossed them with *rhg*/*rhg* mice. Because the

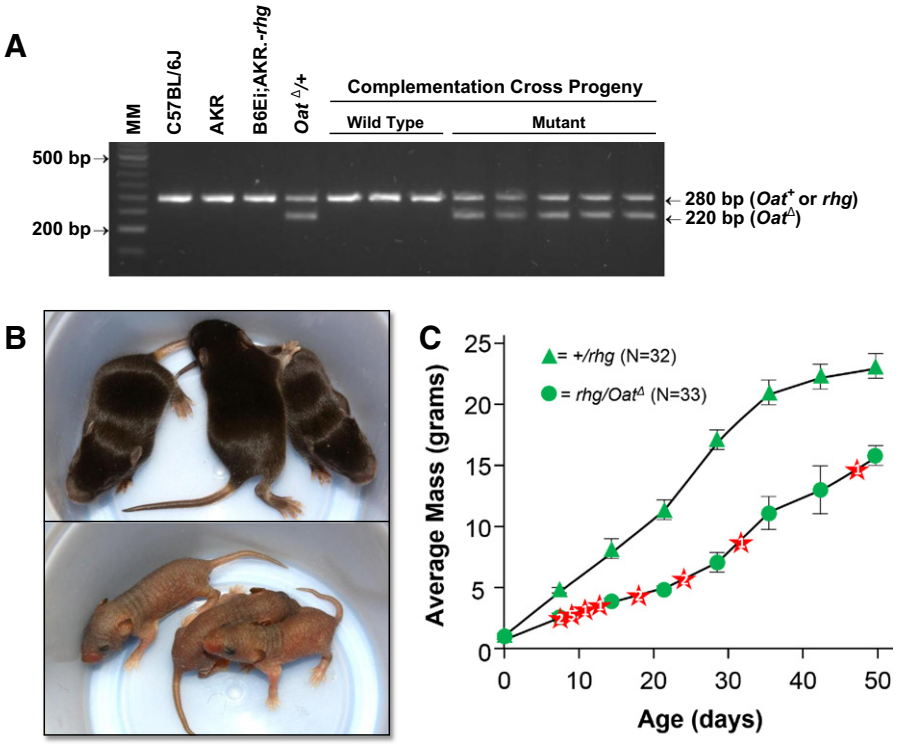

Fig. 4. The recessive Oat^{Δ} null allele fails to complement the recessive *rhg* mutation in compound heterozygotes. (A) Using the 3-primer test described by Wang et al. [17], which generates a 280 bp amplimer from wild type templates or a 220 bp amplimer from Oat^{Δ} templates, 33 *rhg*/Oat^{Δ} mice (and 32 Oat^{+}/*rhg* control siblings) were identified among the progeny of nine *rhg*/*rhg* x Oat^{+}/Oat^{Δ} crosses. (B) While these pups were indistinguishable at birth, by 7 days of age Oat^{Δ} carriers (bottom photograph) displayed the markedly smaller body mass and delayed hair development compared with Oat^{+}/*rhg* controls (top photograph). 10-day-old mice are shown. (C) The average mass (in grams) for as many as 33 Oat^{Δ} carriers and 32 wild type Oat^{+}/*rhg* heterozygotes are shown, ± 1 standard deviation. Red stars show the age and number of mutant mice that died before the end of the 49-day study.

21 mice (out of 34 total progeny) inheriting both *rhg* and *Fgfr2*$^{\Delta}$ were phenotypically normal (in terms of vibrissae morphology and growth rate, see Supplementary Fig. S1) we conclude that these mutant alleles complement, indicating that *rhg* is not an allele of *Fgfr2*.

3.4. High-resolution genetic mapping

To more precisely locate *rhg*, recombinant mice from the backcross panel were next typed for single nucleotide polymorphisms (SNPs) that lie between *D7Mit186* and *D7Mit291*. Supplementary Tables S1 and S2 fully describe the 6 SNP sites that were used. This analysis, summarized in Fig. 3A, identified nine crossovers that positioned *rhg* telomeric of *SNP2*, and three crossovers that placed *rhg* centromeric of *SNP5*. This small region contains less than 910 kb of DNA, and only 10 genes [19] (and see Fig. 3B).

3.5. Sequence analysis of the Oat gene in the rhg mouse

Among those 10 genes, ornithine aminotransferase (abbreviated *Oat*) became a strong candidate because of its known expression in skin [27]. Furthermore, although mice homozygous for an engineered null allele of *Oat* (herein designated *Oat*$^{\Delta}$) die within 24–48 h of birth, when rescued by twice-daily injections with arginine, these mutants show slow postnatal growth compared to their *Oat*$^{\Delta}$/+ littermates [17], similar to *rhg* mutants in testcrosses (see Fig. 1B). We therefore determined the DNA sequence for all coding regions of the *Oat* gene (Fig. 3C) in *rhg*/*rhg*, +/*rhg*, and control wild type mice including strains C57BL/6J, A/J, and AKR/J (the genetic background on which the *rhg* mutation originated). This analysis revealed a single G to C transversion in Exon 9 that creates a *Hae*III restriction endonuclease cut site in *rhg*/*rhg* mutants and destroys a *HhaI* site found in wild type strains (Fig. 3D). PCR products including this site that were amplified from various wild type strain templates were not cleaved with *Hae*III, whereas amplimers copied from *rhg* templates were (Supplementary Fig. S2), suggesting that this single base-pair change is specific to the *rhg* mutation. This base substitution is predicted to change a highly-conserved glycine at position 353 in the OAT protein (see Supplementary Table S4) to an alanine residue, suggesting further that this missense mutation could be the molecular basis of the mutant phenotype in *rhg* mice.

3.6. Complementation testing with Oat$^{\Delta}$

To determine if this missense mutation might disrupt the normal function of the *Oat* gene product in *rhg* mutants, we crossed *rhg*/*rhg* mutants with carriers of the recessive *Oat*$^{\Delta}$ null allele [17]. These crosses yielded 65 offspring that were typed by PCR for the *Oat*$^{\Delta}$ null allele and weighed at seven-day intervals for 7 weeks. DNA typing (Fig. 4A) identified 33 *Oat*$^{\Delta}$ carriers and 32 control siblings, a good fit with the 1:1 ratio expected for a testcross ($\chi^2 = 0.0154$, $P > 0.9$). The *Oat*$^{\Delta}$ carriers, while indistinguishable from wild-type siblings at birth, all showed delayed growth by 7 days of age (see Fig. 4B & C). Hair development was defective, as with *rhg*/*rhg* mutants, but nearly half of the *Oat*$^{\Delta}$ carriers (45%) died before the end of the study. These data suggest that *rhg* and *Oat*$^{\Delta}$ do not complement, indicating that the mutant phenotype of *rhg*/*rhg* mice is likely due to the G to C transversion mutation we have identified in their *Oat* gene.

3.7. Mutant rhg physiology reflects OAT deficiency

If the missense mutation found in the *rhg* mutant's *Oat* gene is responsible for the mutant phenotype, then mutants should display altered enzyme function. In that case, the reaction normally catalyzed by OAT in adults (conversion of ornithine to pyrroline-5-carboxylate, P5C) might be perturbed, resulting in altered plasma ornithine levels in mutants. Indeed, adult *rhg*/*rhg* and *rhg*/*Oat* $^{\Delta}$ mutants show profoundly elevated levels of plasma ornithine (Fig. 5A) (and depressed levels of plasma lysine, Supplementary Fig. S3) that are similar to the levels previously reported for both mice and humans homozygous for recessive defects in *Oat* [17]. (*Note bene*: These previously-published data from ref. [17], Table 2, are included here in Figs. 5A and S3 to facilitate comparison with new measurements for mice with various *rhg* genotypes.)

The flux of the reaction catalyzed by OAT in mouse neonates is instead from P5C to ornithine and is necessary for adequate arginine synthesis [32–35]. If the phenotype seen in *rhg* mutants is indeed due to OAT deficiency (and therefore arginine starvation) then supplementation with arginine might be expected

to rescue normal growth kinetics in mutant mice. We therefore administered arginine by i.p. injection to mice between 3 and 20 days of age and did indeed observe improved weight gain by supplemented mutants (*rhg*/*rhg* and *rhg*/*Oat*$^{\Delta}$) as compared to mutant siblings injected with PBS only (Fig. 5C, E).

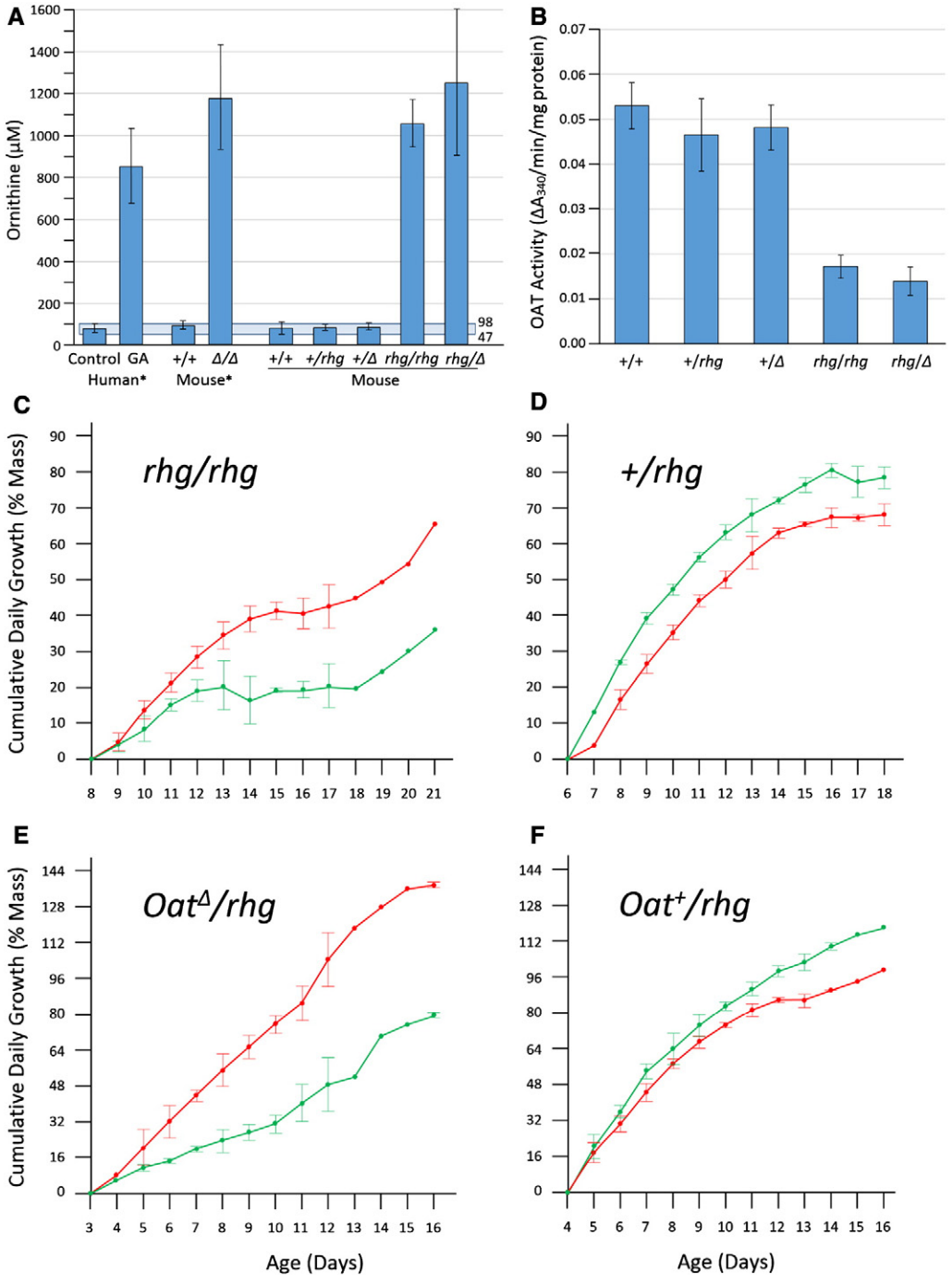

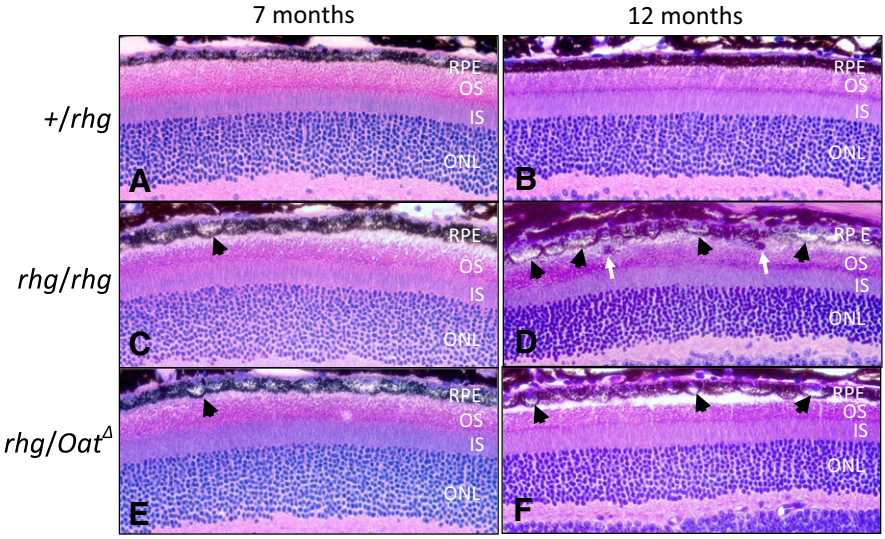

Fig. 6. Light microscopy of the outer layers of 7- and 12-month-old mouse retinas (X400). Retinas of control, 7-month-old (A) and 12-month-old (B) *+/rhg* heterozygotes, illustrating normal retinal pigment epithelium (RPE), photoreceptor outer (OS) and inner segments (IS), and the outer nuclear layer (ONL). Retinas of *rhg/rhg* mutants (C, D) and of *rhg/Oat*$^{\Delta}$ mutants (E, F) are shown at 7 and 12 months of age, respectively. The retinal pigment epithelium in mutant retinas is degenerate, showing abnormal, irregular swelling with frequent doming (black arrowheads). Occasional retinal pigment epithelial cells have migrated into the outer segment layer (white arrows). The photoreceptor outer segments in mutants are somewhat shortened compared to wild type, and are clearly disorganized.

Typically, supplementation with arginine had a slightly negative effect on the growth rates of wild type mice compared with wild type siblings injected with PBS only; see Fig. 5D, F. (Unfortunately, our repeated attempts to rescue *Oat*$^{\Delta}$/*Oat*$^{\Delta}$ mutants to adulthood by arginine supplementation were unsuccessful.) Taken together, the excess of ornithine in mutant adults and apparent deficit of arginine in growing mutant pups suggests that the variant *Oat* allele associated with *rhg* may not function normally.

We therefore investigated OAT activity in *rhg* mutants (and controls) using a continuous coupled assay recently described by Juncosa, Lee and Silverman [23] and modified here to monitor OAT activity in crude liver lysates. Results show that OAT activity is much lower in *rhg/rhg* and *rhg/Oat*$^{\Delta}$ mutants, compared to wild type mice with *+/+*, *+/rhg* or *+/Oat*$^{\Delta}$ genotypes (which were similar to each other; Fig. 5B). These data suggest further that the variant *Oat* allele associated with the *rhg* mutation does disrupt normal OAT function.

Because OAT deficiency is known to cause retinal degeneration in mice [17,21] and in man (see ref. [30], entry #258870), we evaluated histologically the retinas of *rhg/rhg* and *rhg/Oat*$^{\Delta}$ mice, compared to

Fig. 5. Mutant *rhg/rhg* and *rhg/Oat*$^{\Delta}$ mice show hyperornithinemia and reduced OAT activity as adults, and benefit from arginine supplementation as neonates. (A) Plasma ornithine levels of mice tested in this study, compared with levels measured by Wang et al. (1995) for OAT-deficient mice and human patients with gyrate atrophy of the choroid and retina. Plasma ornithine levels marked with an asterisk—from human patients with gyrate atrophy (32 individuals) and controls (30), and from *Oat*$^{\Delta}$/*Oat*$^{\Delta}$ mice (5) and wild type controls (6)—were taken from Wang et al. [17], Table 2. These data are shown for comparison with plasma ornithine levels measured here (in μM) for *rhg/rhg* (6 individuals), *rhg/Oat*$^{\Delta}$ (6), and wild type controls (6 *+/+*, 6 *+/rhg*, and 12 *+/Oat*$^{\Delta}$). The normal range of plasma ornithine in control mice measured here (from 47 to 98 μM) is indicated by the blue-shaded rectangle. (B) Crude liver lysates from *+/+*, *+/rhg*, *+/Oat*$^{\Delta}$, *rhg/rhg* and *rhg/Oat*$^{\Delta}$ mice were tested for OAT activity using a continuous coupled assay based on Juncosa, Lee & Silverman [23]. Average activities are shown in terms of the change in absorption at 340 nm, per mg of total protein in the crude lysate, ±1 standard error. The OAT activity measured for mutant and double-mutant genotypes was significantly reduced compared to that of homozygous or heterozygous wild type mice. (C–F) Pairs of wild-type or mutant mice between 3 and 20 days of age were given twice daily i.p. injections of 0.5 M arginine or PBS, and were weighed daily. Red points show the average cumulative mass gained (expressed as the percentage of the previous day's mass) for arginine-injected subjects, and green is that for PBS-injected controls, ± 1 standard deviation (when three or more weights were available to be averaged). Each panel combines the results of 4 different litters. While wild type mice did not appear to benefit from arginine supplementation (D, F), *rhg/rhg* (C) and *rhg/Oat*$^{\Delta}$ (E) mice with arginine supplementation routinely grew faster than controls.

wild type littermate controls at 7 and 12 months of age. These results (Fig. 6) show that the outer layers of retinas from aged mutants are clearly abnormal, with retinal pigment epithelium cells showing irregularities in size and shape, and some appearing to have migrated into the outer segment layer. Photoreceptor outer segments are also somewhat shortened and disorganized, similar to the rescued $Oat^{\Delta}/Oat^{\Delta}$ mutants described by Wang et al. [17,21]. That the *rhg* mutation clearly controls retinal degeneration—another hallmark of OAT deficiency and a pleiotropic aspect of the *rhg*/*rhg* phenotype not previously known—suggests further that the missense *Oat* mutation we have identified here is the proximal, molecular basis of the spontaneous *rhg* mutant's phenotype.

4. Discussion

We have taken a positional-candidate approach to assign the spontaneous mouse *rhg* mutation to a single G to C transversion in Exon 9 of the mouse *Oat* gene. This mutation appears to be specific to the *rhg* variant, and would cause the substitution of an alanine residue for a glycine that is conserved in 56 animal species surveyed, and in yeast. The failure of an engineered null allele of *Oat* to complement the *rhg* defect in compound heterozygotes confirms this genetic assignment. We therefore recommend that the *rhg* mutation be formally renamed ornithine aminotransferase-*rhg* (Oat^{rhg}).

As its name implies, the spontaneous *rhg* mutant was first discovered on the basis of its delayed development of a hairy coat that is most obvious at 7–10 days of age. We propose that the basis of the *rhg* mutant phenotype in neonates is hypoornithinemia which results in arginine synthesis (via the conversion of ornithine to citrulline in the urea cycle) insufficient to support production of proteins needed for normal growth kinetics in general as well as the development of a hairy coat. Arginine supplementation seems to ameliorate these mutant symptoms, as does the conversion to a solid diet around day 14, supporting this arginine-deficiency hypothesis. Strikingly, human neonates with OAT deficiency (and the expected hypoornithinemia and argininemia in at least in one case; see Wang et al. [17], Fig. 5) have not been reported to show any disease symptoms, or altered hair development. In spite of this stark distinction between mice and humans, the *rhg* mutant could be useful tool for investigating further this crucial role of ornithine metabolism in supporting the normal growth and development of neonatal rodents. It may also provide a model for some conditions in humans, such as protein malnutrition—especially in infants and children (marasmus)—or cases where arginine may be considered essential, as with pre-term infants [36] or with burn or other injuries [37].

The mutant *rhg* phenotype in adult mice includes (at least) cataracts [14] and now hyperornithinemia and retinal degeneration, making it an ideal model for gyrate atrophy of the choroid and retina (GACR, OMIM ID #258870 [30]). The *rhg* mutant might even provide a superior model for GACR compared with Valle's null mutant [17], since *rhg* mutants: 1) live to weaning about 85% (see Fig. 1B) to 90% of the time (see Fig. 2) compared with $Oat^{\Delta}/Oat^{\Delta}$ homozygotes, which die within hours of birth without arginine supplementation (and even with supplementation, in our hands); 2) display plasma ornithine levels very similar to OAT-deficient adult humans and knock-out mice; and 3) have a subtle missense mutation that alters the same, highly-conserved glycine that is substituted in at least one Spanish family with GACR [38]. If a more severe model phenotype is desired by investigators, double heterozygotes (rhg/Oat^{Δ}) can easily be produced and are mostly viable (in that they survive to weaning almost 70% of the time without supplementation; see Fig. 4C).

While both *rhg* mutants and humans with OAT-deficiency share these clinical features (cataracts, hyperornithinemia and retinal degeneration), other pleiotropic, progressive manifestations have been noted for GACR that have not, to our knowledge, been investigated to any degree in mice. These features include type II muscle atrophy [39], early degenerative and atrophic brain changes [40] and cognitive delays [41]. We are hopeful that, with its molecular assignment to the *Oat* gene, the mouse *rhg* mutant can now be used—alone or in combination with Valle's previously-characterized Oat^{Δ} allele—to facilitate the further development of therapies and novel screening assays for GACR.

Supplementary data to this article can be found online at http://dx.doi.org/10.1016/j.ymgmr.2014.08.002.

Acknowledgments

The authors thank undergraduates Nisrine Dagemseh, Michael Desaulniers, Rossmary Rodas, and Saba Chaudhary, and high-school interns Julia Rivera, Kavesha Thakkar, David Hyuckin Lim and Ariel Gilgeours

for help with marker typing; Dr. David Valle (Institute of Genetic Medicine and Departments of Pediatrics, Ophthalmology and Molecular Biology & Genetics; The Johns Hopkins University School of Medicine, Baltimore, MD, USA) for donation of mice carrying the *Oat* knock-out mutation; and Mary Mantzaris for excellent animal care. This work was supported by research grants from Connecticut State University, the Dean of the School of Technology and Engineering, and the National Institute of Arthritis and Musculoskeletal and Skin Diseases of the National Institutes of Health under Award Number R15-AR059572. The content is solely the responsibility of the authors and does not necessarily represent the official views of the National Institutes of Health.

References

[1] D.V. Spacek, A.F. Perez, K.M. Ferranti, L.K.-L. Wu, D.M. Moy, D.R. Magnan, T.R. King, The mouse frizzy (*fr*) and rat 'hairless' (fr^{CR}) mutations are natural variants of protease serine S1 family member 8 (*Prss8*), Exp. Dermatol. 19 (2010) 527–532.
[2] C. Leyvraz, R.-P. Charles, I. Rubera, M. Guitard, S. Rotman, B. Breiden, K. Sandhoff, E. Hummler, The epidermal barrier function is dependent on the serine protease CAP1/*Prss8*, J. Cell Biol. 170 (2005) 487–496.
[3] S. Frateschi, E. Camerer, G. Crisante, S. Rieser, M. Membrez, R.-P. Charles, F. Beermann, J.-C. Stehle, B. Breiden, K. Sandhoff, S. Rotman, M. Haftek, A. Wilson, S. Ryser, M. Steinhoff, S.R. Coughlin, E. Hummler, PAR2 absence completely rescues inflammation and ichthyosis caused by altered CAP1/Prss8 expression in mouse skin, Nat. Commun. 2 (2011) 161.
[4] S. Frateschi, A. Keppner, S. Malsure, J. Iwaszkiewicz, C. Sergi, A.-M. Merillat, N. Fowler-Jager, N. Randrianarison, C. Planès, E. Hummler, Mutations of the serine protease CAP1/Prss8 lead to reduced embryonic viability, skin defects and decreased ENaC activity, Am. J. Pathol. 181 (2012) 605–615.
[5] R. Szabo, K.U. Sales, P. Kosa, N.A. Shylo, S. Godiksen, K.K. Hansen, S. Friis, J.S. Gutkind, L.K. Vogel, E. Hummler, E. Camerer, T.H. Bugge, Reduced prostasin (CAP1/PRSS8) activity eliminates HAI-1 and HAI-2 deficiency-associated developmental defects by preventing matriptase activation, PLoS Genet. 8 (2012) e1002937.
[6] K.J. McElwee, D. Boggess, L.E. King, J.P. Sundberg, Alopecia areata versus juvenile alopecia in C3H/HeJ mice: tools to dissect the role of inflammation in focal alopecia, Exp. Dermatol. 8 (1999) 354–355.
[7] F. Ramirez, A.M. Feliciano, E.B. Adkins, K.M. Child, L.A. Radden II, A. Salas, N. Vila-Santana, J.M. Horák, S.R. Hughes, D.V. Spacek, T.R. King, The juvenile alopecia mutation (*jal*) maps to mouse Chromosome 2, and is an allele of GATA binding protein 3 (*Gata3*), BMC Genet. 14 (2013) 40.
[8] P.P. Pandolfi, M.E. Roth, A. Karis, M.W. Leonard, E. Dzierzak, F.G. Grosveld, J.D. Engel, M.H. Lindenbaum, Targeted disruption of the GATA3 gene causes severe abnormalities in the nervous system and in fetal liver haematopoiesis, Nat. Genet. 11 (1995) 40–44.
[9] J.H. van Doorninck, J. van der Wees, A. Karis, E. Goedknegt, J.D. Engel, M. Coesmans, M. Rutteman, F. Grosveld, C.I. De Zeeuw, GATA-3 is involved in the development of serotonergic neurons in the caudal raphe nuclei, J. Neurosci. 19 (1999) 1–8 (RC12.).
[10] K.C. Lim, G. Lakshmanan, S.E. Crawford, Y. Gu, F. Brosveld, J.D. Engel, Gata3 loss leads to embryonic lethality due to noradrenaline deficiency of the sympathetic nervous system, Nat. Genet. 25 (2000) 209–212.
[11] C.K. Kaufman, P. Zhou, H.A. Pasolli, M. Rendl, D. Bolotin, K.-C. Lim, X. Dai, M.-L. Alegre, E. Fuchs, GATA-3: an unexpected regulator of cell lineage determination in skin, Genes Dev. 17 (2003) 2108–2122.
[12] D. Kurek, G.A. Garinis, J.H. van Doorninck, J. van der Wees, F.G. Grosveld, Transcriptome and phenotypic analysis reveals Gata3-dependent signaling pathways in murine hair follicles, Development 134 (2007) 261–272.
[13] S. Fox, E.M. Eicher, Retarded hair growth (*rhg*), Mouse News Letter 58 (1978) 47.
[14] M. Curtin, L.R. Donahue, P.F. Ward-Bailey, Cataracts and retarded hair growth in *rhg*, MGI Direct Data Submission to Mouse Genome Database (MGD)(J:85256), The Jackson Laboratory, Bar Harbor ME, 2009. (Available from: http://www.informatics.jax.org/).
[15] K. Yu, J. Xu, Z. Liu, D. Sosic, J. Shao, E.N. Olson, D.A. Towler, D.M. Ornitz, Conditional inactivation of FGF receptor 2 reveals an essential role for FGF signaling in the regulation of osteoblast function and bone growth, Development 130 (2003) 3063–3074.
[16] M. Lakso, J.G. Pichel, J. Gorman, B. Sauer, Y. Okamoto, E. Lee, F.W. Alt, H. Westphal, Efficient in vivo manipulation of mouse genomic sequences at the zygote stage, Proc. Natl. Acad. Sci. U. S. A. 93 (1996) 5860–5865.
[17] T. Wang, A.M. Lawler, G. Steel, I. Sipila, A.H. Milam, D. Valle, Mice lacking arnithine-d-amino-transferase have paradoxical neonatal hypoornithinaemia and retinal degeneration, Nat. Genet. 11 (1995) 185–190.
[18] Mouse Genome Database (MGD), Mouse Genome Database Group: The Mouse Genome Informatics website, The Jackson Laboratory, Bar Harbor ME, 2014. (Available from: http://www.informatics.jax.org).
[19] Ensembl Genome Server (EGS), The European Bioinformatics Institute (EBI) and the Welcome Trust Sanger Institute (WTSI), Release 75, Available from: http://www.ensembl.org2014.
[20] W.F. Dietrich, J. Miller, R. Steen, M.A. Merchant, D. Damron-Boles, Z. Husain, R. Dredge, M.J. Daly, K.A. Ingalls, T.J. O'Connor, A comprehensive genetic map of the mouse genome, Nature 380 (1996) 149–152.
[21] T. Wang, A.H. Milam, G. Steel, D. Valle, A mouse model of gyrate atrophy of the choroid and retina, J. Clin. Invest. 97 (1996) 2753–2762.
[22] T. Wang, G. Steel, A.H. Milam, D. Valle, Correction of ornithine accumulation prevents retinal degeneration in a mouse model of gyrate atrophy of the choroid and retina, Proc. Natl. Acad. Sci. U. S. A. 97 (2000) 1224–1229.
[23] J.I. Juncosa, H. Lee, R.B. Silverman, Two continuous coupled assays for ornithine-d-aminotransferase, Anal. Biochem. 440 (2013) 145–149.
[24] A. Orr-Urtreger, M.T. Bedford, T. Burakova, E. Arman, Y. Zimmer, A. Yayon, D. Givol, P. Lonai, Developmental localization of the splicing alternatives of fibroblast growth factor receptor-2 (FGFR2), Dev. Biol. 158 (1993) 475–486.
[25] A. Orr-Urtreger, D. Givol, A. Yayon, Y. Yarden, P. Lonai, Developmental expression of two murine fibroblast growth factor receptors, *flg* and *bek*, Development 113 (1991) 1419–1434.

[26] H.P. Makarenkova, M. Ito, V. Govindarajan, S.C. Faber, L. Sun, G. McMahon, P.A. Overbeek, R.A. Lang, FGF10 is an inducer and Pax6 a competence factor for lacrimal gland development, Development 127 (2000) 2563–2572.
[27] A. Visel, C. Thaller, G. Eichele, GenePaint.org: an atlas of gene expression patterns in the mouse embryo, Nucleic Acids Res. 32 (2004) D552–D556.
[28] C. Li, H. Guo, X. Xu, W. Weinberg, C.-X. Deng, Fibroblast growth factor receptor 2 (*Fgfr2*) plays an important role in eyelid and skin formation and patterning, Dev. Dyn. 222 (2001) 471–483.
[29] S.D. Ferris, R.D. Sage, E.M. Prager, U. Ritte, A.C. Wilson, Mitochondrial DNA evolution in mice, Genetics 105 (1983) 681–721.
[30] Online Mendelian Inheritance in Man (OMIM), McKusick-Nathans Institute of Genetic Medicine, Johns Hopkins University (Baltimore MD), Available from: http://omim.org2014.
[31] D. Valle, O. Simell, The hyperornithinemias, in: C. Scriver, A. Beaudet, W. Sly, D. Valle (Eds.), The Metabolic and Molecular Basis of Inherited Disease, McGraw Hill, Inc., New York, NY, 1995, pp. 1147–1185.
[32] M. Jones, Conversion of glutamate to ornithine and proline: pyrroline-5-carboxylate, a possible modulator of arginine requirements, J. Nutr. 115 (1985) 509–515.
[33] R. Hurwitz, N. Kretchmer, Development of arginine-synthesizing enzymes in mouse intestine, Am. J. Physiol. 251 (1986) G103–G110.
[34] J. Riby, R. Hurwitz, N. Kretchmer, Development of ornithine metabolism in the mouse intestine, Pediatr. Res. 28 (1990) 261–265.
[35] Y. Wakabayashi, E. Yamada, T. Hasegawa, R. Yamada, Enzymological evidence for the indispensability of small intestine in the synthesis of arginine from glutamate. I. Pyrroline-5-carboxylate synthase, Arch. Biochem. Biophys. 291 (1991) 1–8.
[36] G. Wu, L.A. Jeager, F.W. Bazer, J.M. Rhoads, Arginine deficiency in preterm infants: biochemical mechanisms and nutritional implications, J. Nutr. Biochem. 15 (2004) 442–451.
[37] H. Tapiero, G. Mathé, P. Couvreur, K.D. Tew, L-arginine, Biomed. Pharmacother. 56 (2002) 439–445.
[38] L.C. Brody, G.A. Mitchell, C. Obie, J. Michaud, G. Steel, G. Fontaine, M.-F. Robert, I. Sipila, M. Kaiser-Kupfer, D. Valle, Ornithine δ-aminotransferase mutations in gyrate atrophy, J. Biol. Chem. 267 (1992) 3302–3307.
[39] M. Valtonen, K. Nanto-Salonen, K. Heinanen, A. Alanen, H. Kalimo, O. Simell, Skeletal muscle of patients with gyrate atrophy of the choroid and retina and hyperornithinaemia in ultra-field magnetic resonance imaging and computed tomography, J. Inherit. Metab. Dis. 19 (1996) 729–734.
[40] M. Valtonen, K. Nanto-Salonen, S. Jaaskelainen, K. Heinanen, A. Alanen, O.J. Heinonen, N. Lundbom, M. Erkintalo, O. Simell, Central nervous system involvement in gyrate atrophy of the choroid and retina with hyperornithinaemia, J. Inherit. Metab. Dis. 22 (1999) 855–866.
[41] G. Stoppoloni, F. Prisco, R. Santinelli, C. Tolone, Hyperornithinemia and gyrate atrophy of the choroid and retina: report of a case, Helv. Paediat. Acta 33 (1978) 429–433.